Convectively injected water vapor in the North American summer lowermost stratosphere

Michael J. Schwartz,[1] William G. Read,[1] Michelle L. Santee,[1] Nathaniel J. Livesey,[1] Lucien Froidevaux,[1] Alyn Lambert,[1] and Gloria L. Manney[2,3]

Received 25 January 2013; revised 21 March 2013; accepted 26 March 2013; published 29 May 2013.

[1] Anderson et al. (2012) (*A2012*) report in situ observations of convectively injected water vapor (H_2O) in the North American (NA) summer lowermost stratosphere (LMS), occasionally exceeding 12 ppmv. They contend that, in such cold/wet conditions, heterogeneous chemistry on binary water-sulfate aerosols can activate chlorine, leading to catalytic ozone destruction. Aura Microwave Limb Sounder 100 hPa and 82.5 hPa H_2O measurements show that, indeed, the NA LMS is unusually wet, both in mean values and in outliers reaching 18 ppmv. Using *A2012*'s threshold, 4% (0.03%) of 100 hPa (82.5 hPa) NA July–August observations are cold/wet enough for activation. Cold parcels, whether wet or dry, typically have much less HCl to activate and O_3 to destroy than *A2012*'s initial conditions. Slightly lower concentrations of HCl and O_3 in cold/wet parcels are attributable, at least in part, to dilution by tropospheric air. Alarming reductions in NA summer column O_3 suggested by *A2012* are not seen in the current climate. **Citation:** Schwartz, M. J., W. G. Read, M. L. Santee, N. J. Livesey, L. Froidevaux, A. Lambert, and G. L. Manney (2013), Convectively injected water vapor in the North American summer lowermost stratosphere, *Geophys. Res. Lett.*, *40*, 2316–2321, doi:10.1002/grl.50421.

1. Introduction

[2] *Anderson et al.* [2012] (hereafter, *A2012*) report in situ observations of convectively injected water vapor (H_2O) between 120 and 80 hPa in North American summer that reach 12 ppmv, extend horizontally 100 km or more, and persist for several days. These injections are deep into the lowermost stratosphere (LMS), a distinct atmospheric layer of the extratropics between the local tropopause and the 380 K isentrope (corresponding to the tropical tropopause) that has both stratospheric and tropospheric characteristics [*Santee et al*., 2011, and references therein]. At temperatures below 205 K and at aerosol surface area densities of $2\,\mu m^2 cm^{-3}$ typical of this layer [*Deshler et al.*, 2003], such H_2O enhancements produce binary sulfate-water aerosols on which heterogeneous chemistry can activate chlorine to free-radical form, resulting in potentially significant catalytic destruction of ozone (O_3).

[3] Figure 1, adapted from Figure 1 of *A2012*, shows in situ H_2O measurements from the Harvard Lyman-α photofragment fluorescence hygrometer instrument (HWV) as it twice crosses a 1 km layer of 11–12-ppmv H_2O between 105 and 85 hPa. The degree to which the ascent and descent retrace one another in Figure 1c indicates that this layer of enhanced H_2O likely has horizontal extent along the flight path of at least 250 km.

[4] The Microwave Limb Sounder (MLS) on NASA's Aura satellite, launched in 2004, provides daily global atmospheric composition profiles that give context for the sparse in situ measurements. The location where HWV first ascends into the enhanced layer is viewed by MLS 13 h later, but MLS measurements are not consistent with the persistent presence at that location of H_2O at the levels reported by HWV. At 100 hPa (82.5 hPa), MLS retrieves 7.5 ppmv (6.5 ppmv) of H_2O (colored triangles), while convolution of the HWV profile with MLS averaging kernels [*Livesey et al*. 2011] produces 9 ppmv (7.5 ppmv) (black triangles). This difference is significant compared to the $\sim$0.4 ppmv MLS individual measurement precision and 8% estimated accuracy, and may be due to advection and/or dispersion of the enhancement over the intervening 13 h, or error in the inferred spatial extent of the enhancement. Rather than focusing on a single pair of nominally coincident measurements, section 2 capitalizes upon the continuous 8 year MLS record to build a statistical picture of the spatial and temporal distributions of anomalously high H_2O values at 100 and 82.5 hPa, levels spanning *A2012*'s observed enhancements and to which their 90 hPa model results can be applied. Section 3 discusses the joint distribution of temperature and H_2O and the prevalence of conditions sufficient for chlorine activation in North American summer. Section 4 discusses the potential for direct observation of activation signatures in MLS chlorine monoxide (ClO), hydrochloric acid (HCl), and ozone (O_3).

2. High H_2O in the Global LMS

[5] Aura MLS version-3 data products [*Livesey et al*. 2011] provide $\sim$ 3500 profiles per day of atmospheric constituents, including H_2O and O_3 on 12 levels per decade of pressure, and HCl and ClO on six levels per decade in the LMS. This section focuses on H_2O at 100 and 82.5 hPa, MLS retrieval levels that span the layer where *A2012* report high H_2O. The MLS H_2O individual-profile measurement precision at 100 hPa (82.5 hPa) is 0.4 ppmv (0.35 ppmv), and spatial resolution (full width at half maxima (FWHM) of the averaging kernel) is 3 km in the vertical and 200 km

[1]Jet Propulsion Laboratory, California Institute of Technology, Pasadena, California, USA.
[2]NorthWest Research Associates, Socorro, New Mexico, USA.
[3]Department of Physics, New Mexico Institute of Mining and Technology, Socorro, New Mexico, USA.

Corresponding author: M. J. Schwartz, Jet Propulsion Laboratory, m/s 183-701, Pasadena, CA 91109, USA. (michael.j.schwartz@jpl.nasa.gov)

0094-8276/13/10.1002/grl.50421

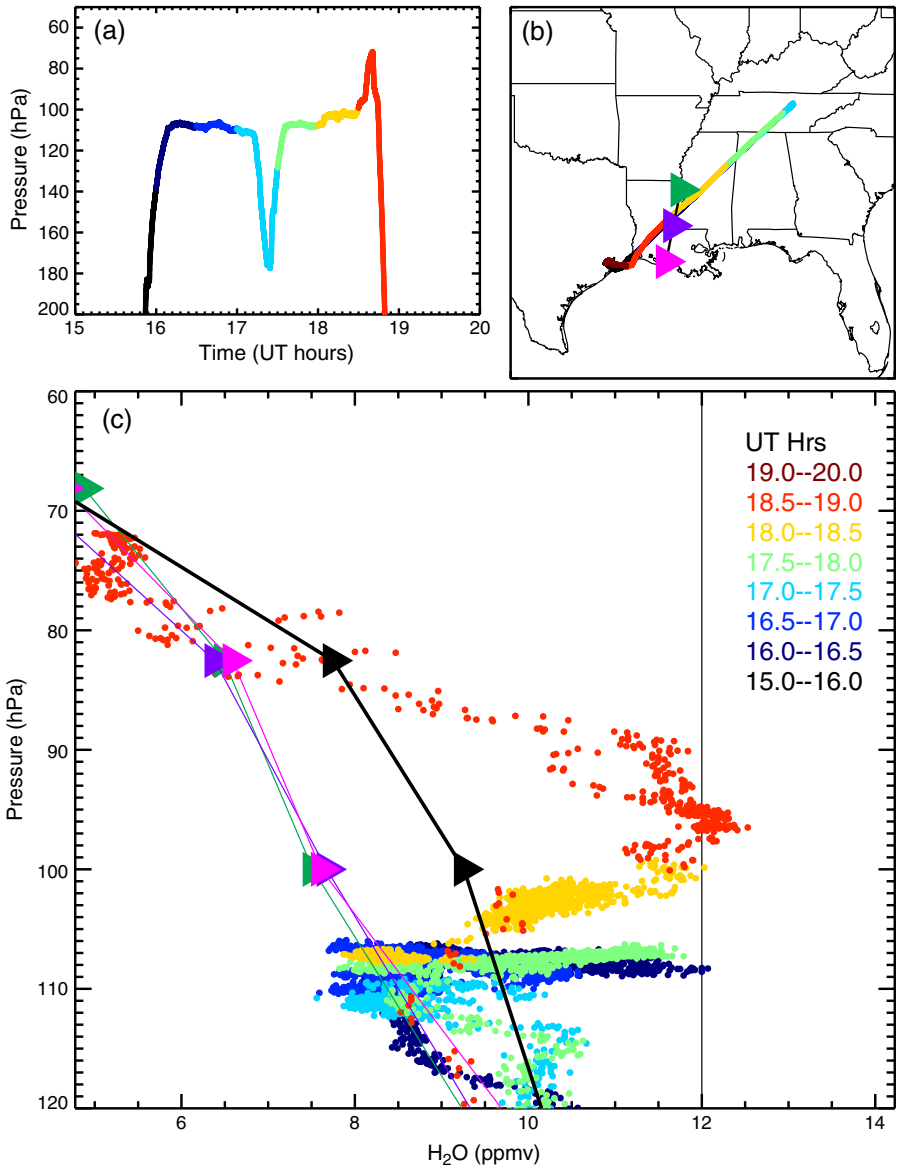

Figure 1. (a) The flight-level pressure profile and (b) the flight track of the 13 August 2007 WB-57 aircraft flight from *A2012*. Color indicates time along the flight path. Near the end of the flight, the aircraft twice crosses a 105–85 hPa layer of elevated H_2O, providing a vertical profile of the enhancement. The locations of the three MLS profiles most nearly coincident with the aircraft observations of enhancement are shown with triangles. (c) H_2O mixing ratios as a function of pressure along the flight track, color-coded by time as in Figures 1a and 1b. The three closest MLS profiles are indicated with lines and triangles colored as in Figure 1b. The black line and triangles are the convolution of the in situ profile with the MLS averaging kernels.

along the orbital-track line of sight. Figure 2a shows the annual-average global distribution of MLS 100 hPa H_2O observations exceeding 8 ppmv, *A2012*'s threshold for rapid activation of chlorine at 200 K with 2 $\mu m^2 cm^{-3}$ of sulfate aerosol. Figure 2b shows the maximum 100 hPa H_2O values observed in each 3° × 5° grid box in the 8 year record. Eastern and southern North America and south central Asia stand out on both plots. The North American box (NA), delineated in green, contains ∼1% of MLS observations, but has 27% of global 100 hPa H_2O observations greater than 8 ppmv, 55% of those greater than 11 ppmv, and 75% of those above 13 ppmv. The frequency with which H_2O exceeds 8 ppmv is highest in the southern part of NA, but Figure 2b shows that the highest individual values, reaching 18 ppmv, occur along the region's northeastern edge.

[6] The Asian monsoon anticyclone region (AMA), delineated in blue on Figure 2, has a larger fraction of global 100 hPa H_2O measurements between 8 ppmv and 10 ppmv than NA, but has fewer extreme outliers above 11 hPa. A small locus of high 100 hPa and 82.5 hPa H_2O outliers on the southeast coast of South America (SA) has a smaller fraction of its H_2O values exceeding 8 ppmv than does NA or AMA, but has some of the most extreme events, with two of the four highest 100 hPa observations and the highest 82.5 hPa observation in the 8 year MLS record. High values in the northeastern Pacific ocean arise from the eruption of

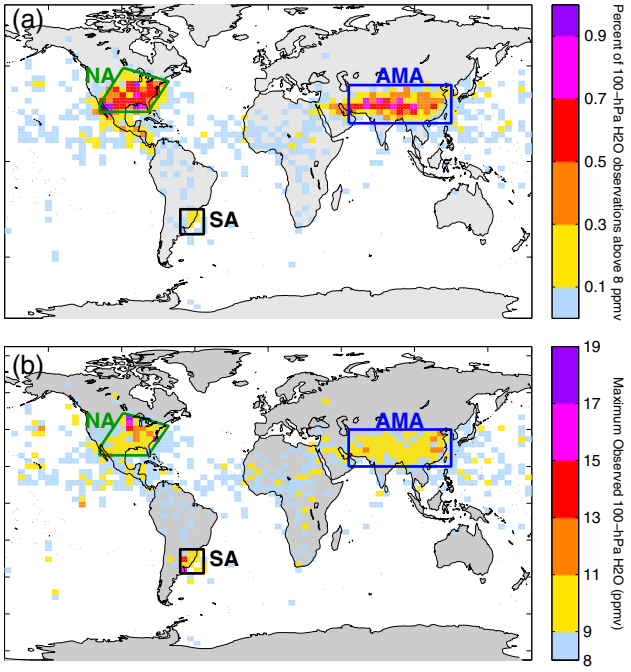

Figure 2. (a) Frequency with which 100 hPa H_2O exceeds 8 ppmv in 8 years of MLS observations. The light-blue color corresponds to one observation in a 3° latitude by 5° longitude bin in the record. (b) The highest 100 hPa H_2O values observed in the 8 year record.

Kasatochi in August 2008. In each of these regions, the highest observed mixing ratios are far outside the 8 year mean distribution, in some cases by more than $10\,\sigma$, but quality metrics show the retrievals to be internally consistent, and the geographic and seasonal (see below) clustering of these measurements argues that, while they are indeed outliers, they are not spurious.

[7] Global, zonally averaged, 100 hPa H_2O at 26°N–49°N (the latitude range of the NA region) has a 1.6 ppmv annual cycle, peaking in September, about an annual mean of 4.5 ppmv, with monthly standard deviations of 0.5–0.8 ppmv. This background is a manifestation of the poleward propagation through the LMS in both hemispheres of a wet anomaly originating in the August–September northern tropics, sometimes referred to as the "horizontal tape recorder" [*Rosenlof et al.*, 1997; *Sandor et al.*, 1998; *Stone et al.*, 2000; *Randel et al.*, 2004].

[8] The 100 hPa time series in the NA region, shown in Figure 3a, has an additional distribution of summer H_2O outliers that peak in the gray-shaded months of July and August. Outlier distributions in AMA and SA also peak in (local) summer, in July–August and January–February, respectively, although the zonal-mean background at the latitude of SA peaks in October. Of the 14 100 hPa H_2O observations that are above 12 ppmv among the 10^7 observations of the global 8 year MLS record, 10 are in the NA box, all but one of which are in July or August and all but one of which are in 2010–2012. Of the other four, two are in AMA in August 2005 and 2007, and two are in SA in January 2010 and February 2012. The clustering of the western-hemisphere outliers in the last 3 years of the record is noteworthy, and there is no indication that non-atmospheric effects, such as instrumental degradation, account for this prevalence.

[9] NA H_2O at 82.5 hPa (not shown) has a 1.2 ppmv peak-to-peak seasonal cycle about a 4.3 ppmv mean, with monthly standard deviations of 0.4–0.7 ppmv. As at 100 hPa, summer outliers at 82.5 hPa peak in July and August, but they are fewer, with values exceeding 6 ppmv less than 1% of the time. In the 10^7 profiles in the 8 year MLS global record, H_2O at 82.5 hPa exceeds 9 ppmv only 18 times: of these, four are in July–August in the NA box, four in April–May in the AMA box, two in January–February in the SA box, and two in the Northeast Pacific in the Kasatochi volcanic plume.

[10] Figures 3b and 3c show the frequency with which MLS H_2O observations in the NA box exceed a given mixing ratio in a given month at 100 and 82.5 hPa. Note that

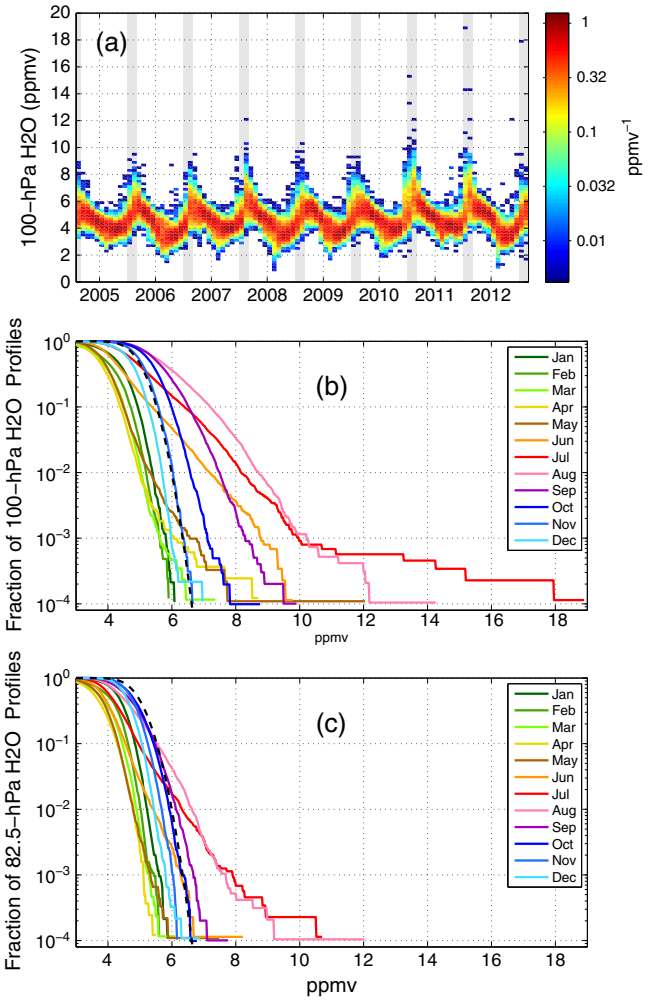

Figure 3. (a) Time series of MLS NA 100 hPa H_2O mixing ratio PDFs. Each monthly histogram is normalized to unity over mixing ratio. Dashed black vertical lines mark year boundaries, and gray-shaded areas denote July–August. (b, c) Monthly probabilities at 100 and 82.5 hPa, respectively, that an NA H_2O observation exceeds a given mixing ratio. For comparison, the black dashed curve repeated on Figures 3b and 3c is a similarly integrated Gaussian with mean value of 5 ppmv and a standard deviation of 0.45 ppmv, consistent with November values at 100 hPa.

these are cumulative probability distribution functions (PDFs), summed from the high side. A cumulative Gaussian comparable to the outlier-free November 100 hPa distribution (black dashes) is shown for comparison. In months in which outliers are significant, non-Gaussian cumulative tails are evident. There are approximately 10^4 NA observations in the 8 year record for a given month, which sets the quantization at the ends of the tails. At 82.5 hPa (Figure 3c), high outliers in NA are only evident in July (0.08%), August (0.06%) and, to a lesser extent, June. Figure 3b shows that 100 hPa, non-Gaussian PDF tails also are largest in July and August, when 1.4% and 3.2% of observations exceed 8 ppmv and 0.4% and 0.6% of observations exceed 9 ppmv, respectively. Outlier tails are first evident in March, and are significant in June and September, when the probability that 100 hPa H_2O exceeds 8 ppmv is 0.3%.

3. Preconditions for Chlorine Activation in the NA Summer LMS

[11] Figure 4a and 4b show the joint PDF of NA, July–August (JA) MLS H_2O and Goddard Earth Observing System version 5 (GEOS-5) temperature (T) [*Rienecker et al.* 2011] at 100 and 82.5 hPa, respectively. Solid curves are chlorine activation thresholds from *A2012* for two sulfate aerosol scenarios: a nominal 2 $\mu m^2 cm^{-3}$ and an enhanced 10 $\mu m^2 cm^{-3}$. *A2012* identify regimes to the left of these thresholds (hereafter, A2 and A10, respectively) as cold and wet enough for more than 10% of chlorine to be converted to active form in the first day after H_2O convective injection. Assuming that the available aerosol surface area is 2 $\mu m^2 cm^{-3}$, and that H_2O enhancements are extensive enough (∼3 km thick) to be resolved by MLS, 4% of 100 hPa and 0.03% of 82.5 hPa NA/JA observations are beyond the activation threshold. Dashed curves include prescaling of an MLS observation to estimate the H_2O mixing ratio within a 1 km layer (enhanced above a nominal 5 ppmv background) that is unresolved by the ∼ 3 km MLS averaging kernels. The fraction of profiles in which the activation threshold could be crossed within some 1 km layer of the 3 km thick volume of air observed by MLS increases to 7% (0.06%) at 100 hPa (82.5 hPa). In the 10 $\mu m^2 cm^{-3}$ enhanced-aerosol case appropriate for volcanic plumes or perhaps for future geoengineering scenarios, activation fractions at 100 hPa (82.5 hPa) are 15% (1%), assuming vertically resolved enhancements, and 19% (2%) if enhanced layers are assumed to be 1 km thick.

[12] Figure 4c shows the percentage of parcels within the NA/JA box that are beyond the activation threshold as a function of latitude. Curves for 100 and 82.5 hPa are shown for nominal 2 $\mu m^2 cm^{-3}$ and elevated 10 $\mu m^2 cm^{-3}$ aerosol levels. As in Figures 4a and 4b,"scaled" thresholds assume that activation occurs in 1 km layers of elevated H_2O that MLS does not completely resolve. The fraction of observations within the activation regime at 100 and 82.5 hPa increases equatorward as the fixed pressure surfaces become closer to the tropopause and less "stratospheric" in nature, colder and wetter but also with less chlorine to activate and less O_3 to destroy. We note that the thermal tropopauses (World Meteorological Organization (WMO) definition, [e.g., *Holton et al.*, 1995]) for profiles with LMS layers within the A2 regime are 113±3 hPa throughout 27°N – 40°N, while the NA/JA zonal means

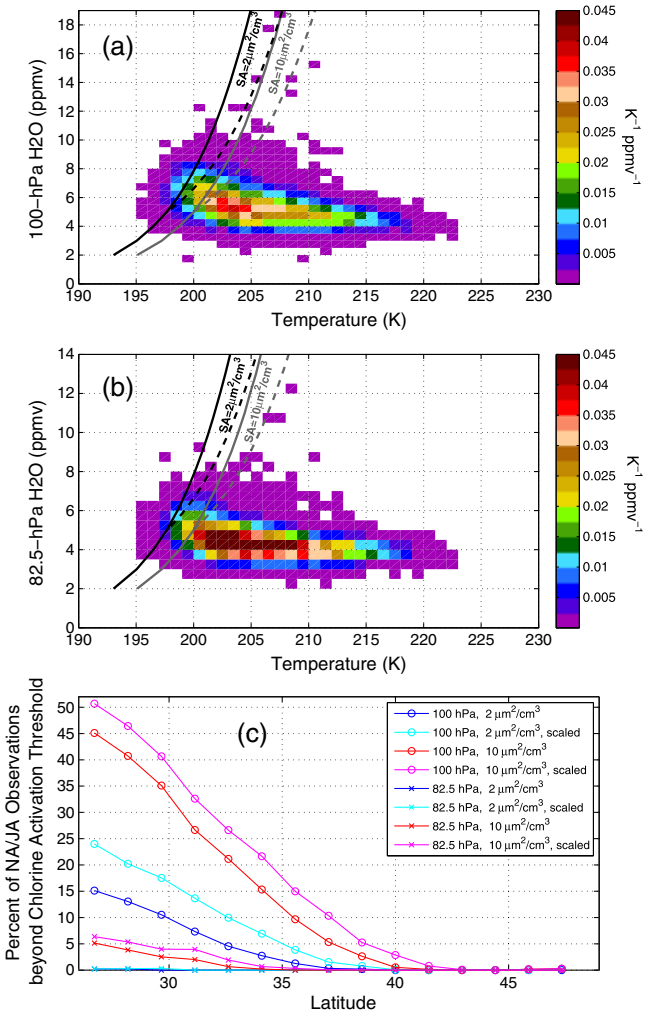

Figure 4. Joint distribution of MLS H_2O and GEOS-5 analysis temperature at (a) 100 hPa and (b) 82.5 hPa for July and August within the NA box. *A2012* assert significant chlorine activation at 90 hPa to the left of the two curves shown for cases of sulfate aerosol surface areas of 10 $\mu m^2 cm^{-3}$ and 2 $\mu m^2 cm^{-3}$. Dashed activation curves are based upon scaled H_2O to give a threshold appropriate within an unresolved, ∼1 km enhanced layer with a profile like Figure 1c, above an ∼5 ppmv background. (c) Percent of NA/JA cases for which the activation threshold is crossed, as a function of latitude within the NA box, for the two pressure levels and two aerosol abundances discussed above.

of observations outside of A2 increase from 119±8 hPa at 27°N to 139±26 hPa at 40°N. The most extreme individual H_2O outliers are in the northern part of the NA box, but the incidence of MLS H_2O observations exceeding 8 ppmv and mean H_2O both increase with decreasing latitude. It is also colder in the southern part of the region, particularly for profiles with high, more tropical tropopauses, and the latitudinal dependence of potential chlorine activation on the fixed-pressure surfaces is primarily determined by the exponential dependence of the activation threshold on temperature. NA/JA mean temperatures at 100 and 82.5 hPa are very similar, both increasing with latitude by 0.7K per degree from 201K at 27°N, and, as can be seen in Figures 4a and 4b, activation is almost never expected above 205K.

4. HCl, ClO and O_3 in the NA Summer LMS

[13] The model run shown in Figure 2b of *A2012* (hereafter, model 2b) assumes initial conditions of 12 ppmv of H_2O, 850 pptv of HCl and 2 $\mu m^2 cm^{-3}$ of sulfate aerosol surface at 200K. HCl drops from 850 to 200 pptv in the first day of activation, and by the end of the second day, daytime ClO increases from near zero to 450 pptv. Over the 4 day model run, O_3 drops whenever ClO is present, falling to 87% of its initial value after 4 days. *A2012* also state that $\sim$ 20% of the total O_3 column lies between 15 and 20 km (123 and 54 hPa) in this region and season.

[14] MLS O_3 and HCl measurements indicate that the NA/JA regions subject to potential chlorine activation have neither as much reservoir chlorine to activate nor as much O_3 to destroy as is assumed in model 2b, even after excluding the potentially depleted A2 regime from these MLS averages. While 18% of total O_3 column is between 15–20 km at the northern edge of the NA box, in the southern part, where conditions necessary for activation are found, only 12% of the O_3 column is between 15–20 km. Furthermore, only 5 $\pm$ 2% of the stratospheric O_3 column (integrated from the WMO tropopause to 1 hPa) is at pressures greater than 82.5 hPa and only 4 $\pm$ 1% is at pressures greater than 82.5 hPa in cases where *T* is less than 205K at either 100 or 82.5 hPa.

[15] MLS NA/JA 100 hPa HCl, with estimated 2 σ accuracy < 200 pptv [*Livesey et al*. 2011], has mean values of 215–450 pptv from south to north in the region. Cases with *T* below 205K but too dry for A2 activation are mostly southern, with mean value of 212 pptv. Interpolating between retrieval levels at 100 and 68 hPa, estimated 82.5 hPa HCl is 355–690 pptv, south-north, but the mean value where *T* is less than 205K and drier than the A2 threshold is 390 pptv. Thus, typical amounts of HCl where activation could occur are less than half of that assumed in model 2b. NA/JA HCl is above 850 pptv when *T* is below 200K in only 0.05% of 100 hPa cases, and in no cases at the interpolated 82.5 hPa level. Furthermore, the A2 and A10 thresholds are defined as *T* H_2O contours on which 10% of inorganic chlorine is activated in the first diurnal cycle after H_2O injection. Model 2b has a 65% conversion of HCl over the first diurnal cycle, and given the non-linearity of the chemistry, it likely has significantly more activated chlorine in the steady state than is realistic for most of the parcels that we have identified as potentially activated.

[16] MLS has two independent version-3 ClO products that provide the potential for direct observation of activated chlorine, but both are subject to biases from interfering spectral features. ClO rapidly converts to ClOOCl at night, with model 2b settling into a diurnal cycle with 450 pptv in daytime and 70 pptv at night, so using observed day-night differences can remove biases that do not have a diurnal cycle. Above 200K, there is increasing nighttime ClO present, so day-night differences become a smaller fraction of daytime abundances. Assuming that model-2b ClO is proportional to initial HCl, we expect that if chlorine were activated as in model 2b, NA/JA A2 day-night differences would be $\sim$200 pptv. However, given the MLS ClO 3 km $\times$ 500 km spatial resolution, diurnal signatures from a 1 km $\times$ 200 km activated layer would be reduced to $\sim$30 pptv. Unfortunately, inconsistency between the two 100 hPa measurements indicates that, in the absence of further validation or retrieval development, the accuracy of the 100 hPa ClO day-night differences should be taken to be $\sim$100 pptv. This degree of accuracy is certainly sufficient to show that activation is not taking place at levels found in the polar winter vortices, where mixing ratios reach 1500–2000 pptv and where activated volumes are large compared to the MLS spatial resolution, but it is not sufficient to make definitive statements about activation at the levels posited in *A2012*.

[17] HCl and O_3 both have large vertical and latitudinal gradients, so care must be taken in computing mean differences of their abundances inside and outside (I-O) of an activation regime. Binning first by *T* and subsequently averaging *T*-binned I-O allows us to isolate the effects of increased H_2O from background conditions that have gradients with respect to *T*. At 100 hPa, average *T*-binned A2 I-O for O_3 is –10 $\pm$ 3 ppbv (–3 $\pm$ 1%). The 100 hPa HCl difference is –7$\pm$12 pptv (–3$\pm$5%). At 82.5 hPa, there are only six profiles within the A2 regime, but if we relax the activation requirement to A10, the mean O_3 difference is –41 $\pm$ 6 ppbv (–6 $\pm$ 1%). The mean interpolated 82.5 hPa HCl I-O for the A10 regime is –26 $\pm$ 12 pptv (–6 $\pm$ 3%). Even if we assume that we are looking for activation in 1 km $\times$ 200 km layers that fill only a fifth of the 3 km $\times$ 350 km HCl averaging kernel, it is clear that MLS does not routinely observe decreases in HCl of 75%, as seen in model 2b. Reductions of O_3 within such a 1 km activated layer might be 3.5 times larger than MLS reports due to the 2.5 km $\times$ 300 km spatial resolution of the O_3 measurement, but inferred column losses are insensitive to whether or not the depleted layers are resolved. While the O_3 deficits within the activation regime are not inconsistent with a small amount of chemical loss, some portion of the inferred depletions must be attributed to dilution by the convective injections of tropospheric air that supply the high H_2O.

5. Summary and Implications

[18] At 100 and 82.5 hPa, the North American (NA) summer has among the highest mixing ratios of H_2O in the global 8 year MLS record, both in terms of monthly mean values and in extreme values. *A2012* report convectively injected H_2O in the LMS, at least at some point, during half of flights planned to observe outflow from convective storms in the US summer. MLS is expected to measure 9 ppmv when observing a 1 km thick, 12 ppmv layer such as the one shown in *A2012* and repeated here in Figure 1. Only 2.5% of MLS NA July–August (JA) 100 hPa mixing ratios are greater than 8 ppmv and 0.5% are greater than 9 ppmv. Thus, while there may be small volumes with higher mixing ratios immediately following convective injections, as these enhancements spread horizontally to 100 km scales, they are only present with H_2O above 12 ppmv 0.5% of the time, even if their layer thickness remains $\sim$ 1 km.

[19] Assuming 2 $\mu m^2 cm^{-3}$ of sulfate aerosol surface area, at the 26°N southern edge of the NA study box it is cold enough and wet enough to promote chlorine activation 15%–25% of the time at 100 hPa, depending on the assumptions made for the size of the parcels relative to the volume of the MLS averaging kernel. At 82.5 hPa, only 12 of $\sim$20,000 NA/JA observations are within the 2 $\mu m^2 cm^{-3}$ (A2) activation regime, even if H_2O is scaled up under the assumption that enhancements are confined within 1 km layers. The NA/JA latitudinal dependence of activation is largely

determined by the meridional temperature gradient. There are almost no cases beyond the activation threshold poleward of 37°N at 100 hPa and none poleward of 30°N at 82.5 hPa.

[20] *A2012* assume 850 pptv of HCl in the background conditions for their simulation but, where temperatures are below 205K (so conducive to activation if wet enough) but outside of the A2 regime (so not previously depleted of HCl), mean MLS 100 hPa HCl is 207 pptv and mean (interpolated) 82.5 hPa HCl is 390 pptv. Thus model 2b almost certainly over-predicts current chlorine activation and O_3 loss rates. Definitive observation of ClO would be a clear indicator of activation, but the two MLS ClO products are inconsistent, suggesting an uncertainty in 100 hPa measurement accuracy of $\sim$100 pptv and precluding definitive confirmation of the chlorine activation posited in *A2012*.

[21] At 100 hPa, NA/JA HCl is lower by 3 ± 5 % and O_3 is lower by 3 ± 1 % within the A2 activation regime than in drier parcels at the same temperature. At 82.5 hPa there are only six NA/JA observations cold and wet enough to be in the A2 activation regime, but within the slightly drier A10 regime, O_3 is lower by 6 ± 1 % and interpolated HCl is lower by 6 ± 3 % than in still drier parcels at the same temperature. These differences are consistent with some degree of chlorine activation and chemical O_3 loss in the activation regimes, but depletions are small compared to model predictions from Figure 2b of *A2012*, even if activation were taking place only in unresolved, 1 km x 200 km layers, and some portion of the reduction must be attributed to dilution of LMS abundances by the convectively injected tropospheric air that supplied the high H_2O.

[22] These processes certainly warrant further study, both from observational and modeling perspectives. Correlative observations of reactive chlorine molecules would be useful, particularly in addressing ambiguity in the MLS LMS ClO measurements. However, injection of H_2O into the LMS only occurs to a significant extent in the upper-level anticyclones associated with the NA and Asian monsoons and, in the 8 year MLS record, there is no indication of alarming depletion of O_3 over NA triggered by these injections of H_2O. *A2012*'s suggestion that NA summer O_3 column is currently significantly threatened is not supported, but a changing climate with a colder LMS, more intense convection or increased aerosol (perhaps from geoengineering) could elevate the importance of the *A2012* mechanisms.

[23] **Acknowledgments.** We thank GMAO and the HWV science team for data sets used. Work at the Jet Propulsion Laboratory, California Institute of Technology, was carried out under contract with NASA.

[24] The Editor thanks two anonymous reviewers for their assistance in evaluating this paper.

References

Anderson, J. G., D. M. Wilmouth, J. B. Smith, and D. S. Sayres (2012), UV dosage levels in summer: Increased risk of ozone loss from convectively injected water vapor, *Science*, *337*(6096), 835–839, doi:10.1126/science.1222978.

Deshler, T., M. E. Hervig, D. J. Hofmann, J. M. Rosen, and J. B. Liley (2003), Thirty years of in situ stratospheric aerosol size distribution measurements from Laramie, Wyoming (41°N), using balloon-borne instruments, *J. Geophys Res.*, *108*, D5, doi:10.1029/2002JD002514.

Holton, J., et al. (1995), Stratosphere-troposphere exchange, *Rev. Geophys.*, *33*, 403–439.

Livesey, N., et al., (2011), EOS MLS version 3.3 level 2 data quality and description document, *Technical Report*, Jet Propulsion Laboratory, California Institute of Technology, Pasadena, California.

Randel, W., F. Wu, S. Oltmans, K. Rosenlof, and G. Nedoluha (2004), Interannual changes of stratospheric water vapor and correlations with tropical tropopause temperatures, *J. Atmos. Sci.*, *61*(17), 2133–2148, doi:10.1175/1520-0469.2004.061.

Rienecker, M. M., et al. (2011), MERRA: NASA's modern-era retrospective analysis for research and applications, *J. Climate*, *24*(14), 3624–3648, doi:10.1175/JCLI-D-11-00015.1.

Rosenlof, K. H., A. F. Tuck, K. K. Kelly, J. M. Russell III, and M. P. McCormick (1997), Hemispheric asymmetries in water vapor and inferences about transport in the lower stratosphere, *J. Geophys. Res.*, *102*, 13,213–13,234, doi:10.1029/97JD00873.

Sandor, B. J., W. G. Read, J. W. Waters, and K. H. Rosenlof (1998), Seasonal behavior of tropical to mid-latitude upper tropospheric water vapor from UARS MLS, *J. Geophys Res.*, *103*, 25,935–25,947, doi:10.1029/98JD02272.

Santee, M. L., G. L. Manney, N. J. Livesey, L. Froidevaux, M. J. Schwartz, and W. J. Read (2011), Trace gas evolution in the lowermost stratosphere from Aura Microwave Limb Sounder measurements., *J. Geophys. Res.*, *116*, D18306, doi:10.1029/2011JD015590.

Stone, E. M., L. Pan, B. J. Sandor, W. G. Read, and J. W. Waters (2000), Spatial distributions of upper tropospheric water vapor measurements from the UARS Microwave Limb Sounder, *J. Geophys. Res.*, *105*, 12,149–12,161, doi:10.1029/2000JD900125.